IOSR Journal of Applied Chemistry (IOSR-JAC)
e-ISSN: 2278-5736.Volume 14, Issue 9 Ser. I (September 2021), PP 16-22
www.iosrjournals.org

Ce-doped Nb_2O_5; Synthesis and Ethanol Sensing Properties

S.V. Jagtap[1], S.D. Thakare[1], A.S. Tale[1], M.J. Pawar[2*]
Department of Physics, RDIK College, Badnera Rly, Amravati-444701M.S. India
Laboratory of Materials Synthesis, Department of Chemistry, Smt. Narsamma ACS College, Kiran Nagar, Amravati-444606 M.S. India

Abstract
Nb_2O_5 nanoparticles have been successfully synthesized via a hydrothermal process. In the reaction process, the commercial Nb_2O_5 powder, H_2O_2 and NH_3 aqueous solutions have been used as precursors. The crystallographic phases, optical and vibronic properties were examined by X-ray diffraction (XRD) and FT-IR spectroscopic methods. Morphology of the produced samples was studied using a scanning electron microscope (SEM). From the X-ray diffraction patterns, it suggested that the product was well crystallized and had the crystal structure oforthorhombic phase of Nb_2O_5.The average crystallite sizes of nanoparticles were calculated by applying the Debye-Scherrer formula and was 27-31 nm. Transmission electron microscopy (TEM) studiesillustrate that both the pure and Ce-doped Nb_2O_5samples withan average diameter of 28-35 nm, which is in good agreement with the average crystallitesizes calculated by Scherrer's formula.It wasobserved that both of the pure and Ce-doped Nb_2O_5 after calcination at 450˚C exhibited tremendous gas sensing performance toward ethanol.Gas sensing properties showed the selectively higher response for 400 ppm ethanol gas at an operating temperature of 200˚C.

Keywords*: Nb_2O_5; Ce-doped Nb_2O_5; Ethanol sensor; Hydrothermal Synthesis;*

Date of Submission: 07-09-2021 Date of Acceptance: 22-09-2021

I. Introduction

With the development of science and technology, ethanol gas sensors have been widely applied in chemical industries and in day to day life. Ethanol sensors with effective and selective sensitivity are extensively used by traffic police to detect drunken drivers, in wine industries for controlling the fermentation process, food package testing, different medical applications etc.

Due to the increase in environmental pollution and health hazards there is an increase in the demand for efficient chemical sensors to monitor environment [1-3]. Also, sensors are now considered as promising candidate for human exhale breath analysis to monitoring diseases. Acetone, alcohol, ammonia and so on, are some of the volatile organic compounds (VOCs) present in our breath [4-6]. So, based on their elevated concentration in breath lots of diseases can be diagnosed which is very important to monitor human health [7-9]. Among these VOCs ethanol is one of the widely studied pollutants. Accurate ppm level ethanol detection is quite difficult. Detection of ethanol vapor is very important for traffic police to detect drunken drivers, to control the fermentation process, etc. However, detection of a single target analyte amidst 1000 other volatiles (some of which could be cross-interfering) remains a challenge for the researchers. GC-MS, ion spectrometry etc. are traditional gas analysis tools. However, they are costly sophisticated and requires skilled manpower for operation. Need of the hour is metal oxide semiconductor based gas sensor which can be used as a breath analyzer.

Metal oxide semiconducting nanoparticles are considered to be the most efficient and promising material for gas sensors due to the presence of higher oxygen vacancies and surface area [10-12].Like other metal oxides such as titanium dioxide (TiO_2) and zinc oxide (ZnO),Nb_2O_5 has shown great potential to be used as a sensing material. Niobium oxide films have been widely used for a wide variety of technological applications such as sensing materials and biocompatible coatings [13–15], optical and electronic devices [16], catalysts [17, 18], ion exchange materials, energy storage electrode material for lithium batteries and solar cell applications [19, 20].

Sensor devicesbased on Nb_2O_5 for gas, humidity, biological and chemical sensing as well asphotodetection have been successfully demonstrated. Generally, the main parametersfor good sensing device performance are the size, morphology, aspect ratio,intergranular connectivity, porosity, surface energy, stoichiometry and surface areato volume ratio of the incorporated sensing material.

In this work, we have synthesized Nb_2O_5 based gas sensor to improve the gas sensing properties of sensor for ethanol. We have performed a series of gas sensing examination of the synthesized material. And the results indicate the Ce-doped Nb_2O_5 own excellent gas sensing performance (high sensitivity, good selectivity, rapid response and recover rates, and long stability) to ethanol at low working temperature. The high gas sensing performance is caused by the large surface area of the material, which makes the detected gas and material contact very well and extremely improves the gas sensing performance of the as-obtained materials.

II. Experimental

2.1 Material Preparation

Pure and Ce-doped Nb_2O_5nanoparticles with variable concentration of Ce (0 wt%, 2wt% and 4 wt%) have been prepared by using hydrothermal method. Niobium pentachloride ($NbCl_5$), Liquid ammonia (NH_3), Potassium permanganate ($KMnO_4$), Sodium nitrate($NaNO_3$) and hydrogen peroxide (H_2O_2) were purchased from Merck Chemicals. The Cerium (III) chloride heptahydrate (99.9% Sigma Aldrich) was used as a source of Ce. All chemicals were used as received without any further purification.

Niobium pentachloride was dissolvedin 40 ml of water was mixed in a flask with ammonia and H_2O_2 solution in calculated amount. To this mixture, a calculated amount of cerium (III) chloride was added. The mixedsolution was placed in a Teflon-sealed autoclave. The hydrothermalsynthesis was carried out at 400 K while the bottle wascontinuously rotated at a speed of 50 rpm. The typical synthesis time was 36 h. After the synthesis, the formation of a solid precipitate was observed at the bottom of the autoclave.Theprecipitate was calcined in air byusing a furnace at 723 K for 3 h and sample coding is done as in Table 1.The prepared powders were processed for thick film preparation to investigate the gas sensing properties.

2.2 Thick film fabrication

The milled powder of the prepared samples was mixed with an organic vehicle (OV) consisting of 15% ethylcellulose (EC) and 85% terpineol to form a paste. The paste was screen printed on an alumina substrate using screen printing technique employing a 190 mesh screen to form a thick film. Before screen printing the sample paste, the alumina substrate was provided with silver electrode using the screen printing method. The film was then sintered at 600˚C for 4 hour.

2.3 Characterization

The crystalline structure of both pure and Ce-doped Nb_2O_5nanoparticles was characterized by X-ray powder diffraction (XRD).Powder XRD patterns were recorded on a Philips diffractometer (PW1800, CuKαradiation, graphite monochromator). Particle shape and product morphology were characterized by scanning electronmicroscope (SEM). Measurements of the surface area of the dry powder were done by nitrogen adsorption–desorptionisothermal analysis.

III. Results and Discussion

3.1 XRD

Figure 1 represents the XRD patterns for the pure and Ce-doped Nb_2O_5 samples annealed at 450˚C. While no obvious peak is seen on the XRD patterns of pure and doped Nb_2O_5annealed at 450˚C, which would indicate a crystalline phase which confirms the presence of the orthorhombic Nb_2O_5 in both pure and Ce-doped Nb_2O_5 samples. The sharp reflections of pure and Ce-doped Nb_2O_5 samplescan be well indexed as the (200), (201), (002), (380) and (202) planes of the orthorhombic phase of Nb_2O_5 structure. A broad peak at about 2θ = 25˚ indicates the Nb_2O_5 crystallite sizes are too small to be detected [21]. The average crystallite size was calculated by applying the Debye–Scherrer formula on the hexagonal (001) diffraction peaks and are found in the range of 27to 31 nm for pure and Ce-doped Nb_2O_5samples. The difference in the average crystallite size is not remarkable even on the doping of Ce from 2wt% and 4wt% in Nb_2O_5 structure. The XRD patterns pure and Ce-doped Nb_2O_5samples possess no secondary phase. The lattice parameters of pure and Ce-doped Nb_2O_5samplesshow similar results (Table 1).

Table 1 Ce wt%, average crystallite size and lattice parameters values of pure and Ce-doped Nb_2O_5.

Sample	Ce wt%	Average crystallite size (nm)	Lattice parameter values(Å)		
			a	*b*	*c*
NbO	0	30.33	6.162	29.313	3.930
C2NbO	2	27.42	6.165	29.354	3.933
C4NbO	4	28.22	6.172	29.359	3.936

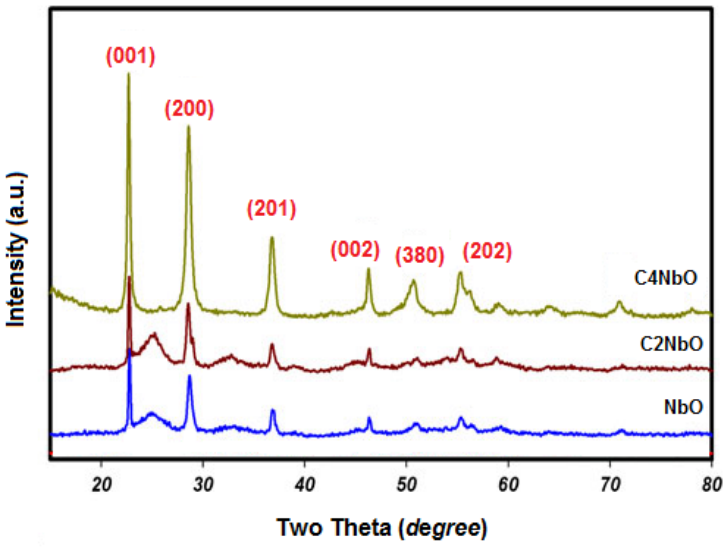

Figure 1 XRD patter of pure and Ce-doped Nb_2O_5.

3.2 SEM and TEM studies

Figure 2(a) shows the SEM micrographs of Ce-doped Nb_2O_5samplesby the hydrothermal method, at a temperature of 450°C. The samples show the nanoparticles formation.From Figure 2, one can observe that, the surface of C2NbO sample is porous and larger which is suitable for the maximum adsorption of the target gas molecules. Further confirmation was done with the help of transmission electron microscopy (TEM) Figure 2(b) shows the transmission electron micrograph ofC2NbO sample.The average crystallite size of the prepared samples is in the range of 28-35 nm and are in good agreementwith thecrystallite size estimated by XRD method.

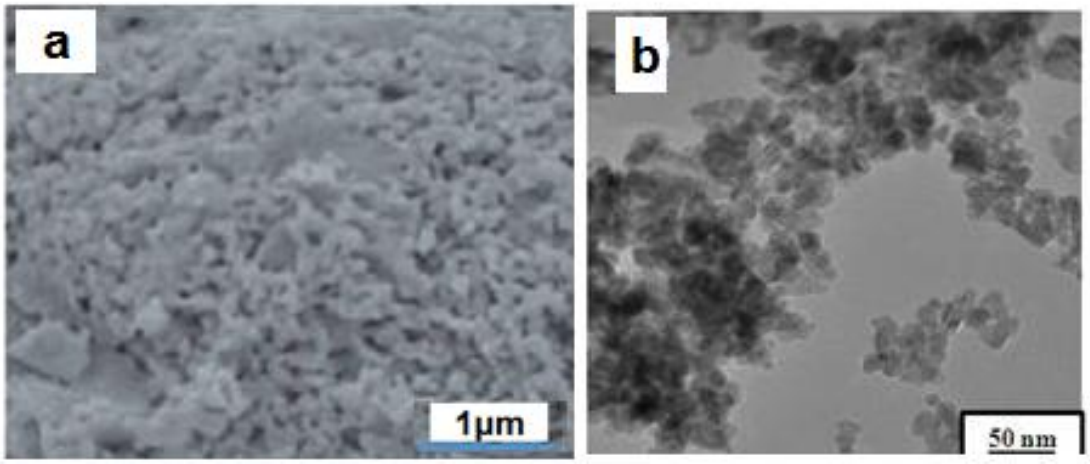

Figure 2(a-b) SEM and TEM images of C2NbO sample.

3.3 FT-IR studies

The vibrational modes of Ce-doped Nb_2O_5 samples were studiedbyIRspectroscopywithinthewavenumberrangeof3000–500cm^{-1}.Inthespectrumpresented in Figure3, neither band was associated to the presence of organic components nor were found pronounced shoulders related to the amorphous phase of niobium pentoxide. The shoulder around 771 cm^{-1} for the sample at 2.0 wt% Ce content is characteristic of the orthorhombic structure of niobium pentoxide. The absorption bands observed at 689 cm^{-1} for 4.0 wt% may correspond to the coupling mode of vibration of Ce-O stretching in octahedral sites of Ce-doped Nb_2O_5. The band observed at 1660 cm^{-1} is attributed to vibrations of the surface adsorbed O-H molecules [21].

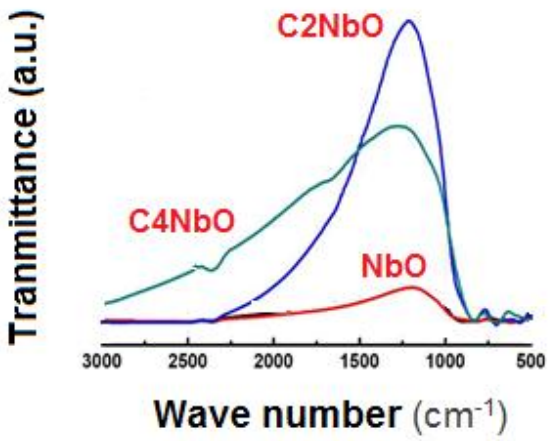

Figure 3 FT-IR spectra of pure and Ce-doped Nb_2O_5.

IV. Gas response

The relative response (*S*) for a target gas is determined as the ratio of the change in conductance of a sample upon exposure of the target gas to the original conductance in air. The relation for *S* is given as –

$$S = \frac{G_g - G_a}{G_a}$$

whereG_a is the conductance in air and G_g the conductance in a target gas.

Figure 4a shows the variation of ethanol responses of pure and Ce-doped Nb_2O_5samples with operating temperature. The gas concentrations are taken from 100 ppm to 400 ppm with an increasing level of 100 ppm. The responses of pure and Ce-doped Nb_2O_5thick film to ethanol were observed to increase with operating temperature reach to their respective maxima and then decreased with further increase in operating temperature. The responses of pure Nb_2O_5 to ethanol were found to be 18% at150°C. The lower sensitivity at low temperature to a particular gas against different gases is the main drawback of pure Nb_2O_5 thick films.

At 150˚C, for 100 ppm ethanol gas concentration, C2NbO sensor showed 63.4% of sensing response and at 400 ppm, the sensing response is recorded to be 77.9%. At the same temperature condition, for 100 ppm ethanol gas, the C4NbO sensor showed 27% of sensing response and at 400 ppm, the recorded sensing response is 54.9%.In Ce-doped Nb_2O_5, the response is found to be systematically rising with Ce doping concentration upto 2wt%. But when concentration of Ce exceed 2wt%, the response get fall down. With the doping concentration its ethanol response and operating temperature decreases. 2wt% Ce-doped Nb_2O_5exhibits the highest response of 91.3 % at 200˚C for 400 ppm ethanol.

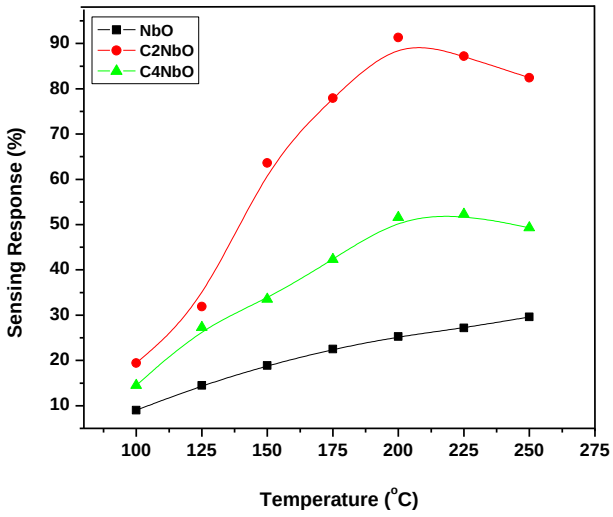

Figure 4aEthanol gasresponse of pure and Ce-doped Nb_2O_5 as a function of temperature [Ethanol gas concentration = 400 ppm].

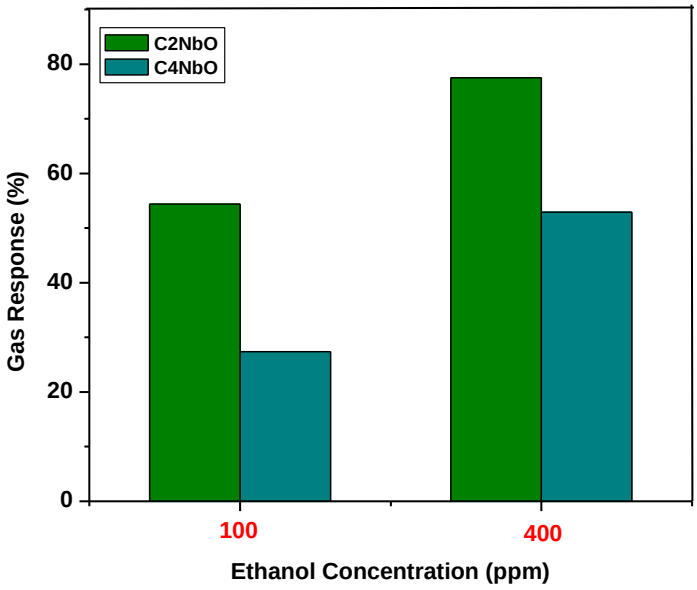

Figure 4b Ethanol gas response of Ce-doped Nb_2O_5 as a function of ethanol gas concentration at 150˚C.

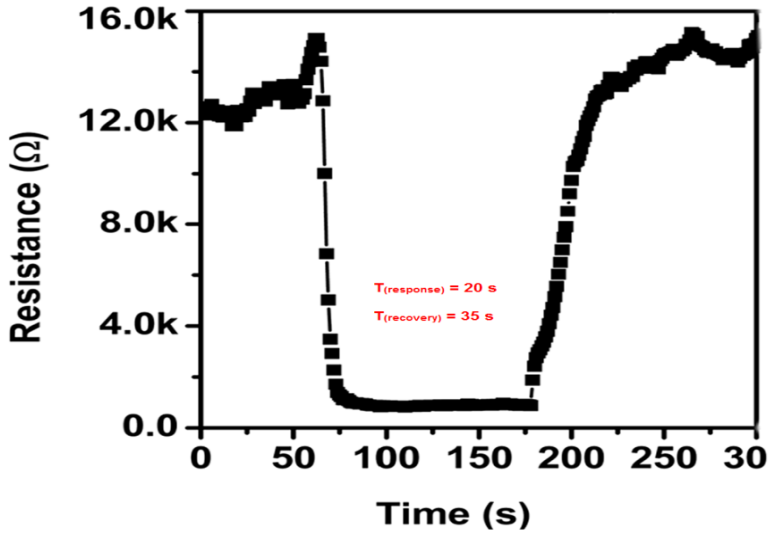

Figure 5 Response and recovery time of the C2NbO sensor to 400 ppm ethanol at operating temperature 200˚C.

The response-recovery behavior is also vital characteristic parametersfor gas sensors. It was defined as the time needed for thesensor-resistance to change by 90% of the difference from the maximumafter injecting and removing the detected gas. It can be clearlyobserved that the response of Ce-doped Nb_2O_5 sensor increasedabruptly after the injection of ethanol and decreased rapidly, thenrecovered to its initial value after the test gas was released. Theresponse and recovery time are about 20 and 35 s for ethanol, as shownin Figure 5.

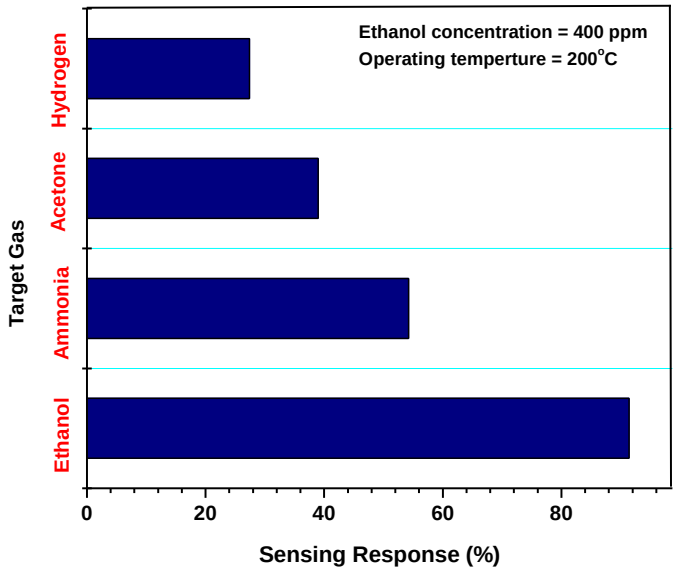

Figure 6Selectivity of C2NbO sensor for different target gases with same concentration at operating temperature 200˚C.

Selective detection of the target gas remains a challenge for theapplication of metal oxide semiconductor based gas sensor [22]. Toidentify the selectivity of the three sensors, the cross response propertiesof the sensors were examined by exposing the sensors to400 ppm ethanol and other gases like ammonia, acetone and hydrogen at 200˚C, as summarized in Figure 9. Itwas seen that the response of Ce-doped Nb_2O_5sensor to 400 ppmethanol is much higher than that of other sensors. The response canreach to 91%, which was about two times higher than the response ofammonia and more than four times than that of other gases, indicatingan excellent selectivity to ethanol.

Mechanism of gas sensing performance

The ethanol sensing mechanism of the sample is explained asfollows. Adsorption is a surface defect. It forms the ionic species($O_2^-$and O^-) on sample surface. Kinetic reaction before and afterthe ethanol exposure is described in the equations (I)–(III).

$$O_{2(gas)} \leftrightarrow O_{2(adsorbed)} \quad \text{(I)}$$

$$O_{2(adsorbed)} + e^- \leftrightarrow O_{2\,(adsorbed)}^- \quad \text{(II)}$$

$$O_{2\,(adsorbed)}^- + e^- \leftrightarrow 2O_{(adsorbed)}^- \quad \text{(III)}$$

Before exposure to organic gas, oxygen atoms are adsorbed intoNb_2O_5 surface and it takes electrons from surface and become O^-. This O^- ion helps to create the depletion layeron the host surface. Addition of double doping element help tocompletes the Nb_2O_5 structure. This allows more oxygen to beadsorbed and increased the surface area which can enhance the sensing response.

V. Conclusion

In summary, a simple hydrothermal method has been developed forpreparing pure and Ce-doped Nb_2O_5 nanostructures. It was found thatthe Ce doping plays an important role in controlling themorphologies and structures of the products. The as-preparednanostructures were used as the efficient gas sensing materialsto detect flammable and explosive gas like ethanol. The Ce-doped Nb_2O_5 gas sensor exhibits highly sensitiveand selective sensing properties to ethanol gas. The responsecan reach to 91 for 400 ppm ethanol which is much higher thanthat of pureNb_2O_5. Thiswork demonstrates that the simply prepared Ce-doped Nb_2O_5nanostructures have a potential application in ethanol gas sensor.

References

[1]. Wang, L. L., Fei, T., Lou, Z., and Zhang, T. (2011a). Three-dimensional hierarchical flowerlike -Fe_2O_3 nanostructures: synthesis and ethanol-sensing properties. *ACS Appl. Mater. Interfaces* 3, 4689–4694.

[2]. Chao, J. F., Xu, X., Huang, H. T., Liu, Z., Liang, B., Wang, X. F., et al. (2012). Porous SnO_2 nanoflowers derived from tin sulfide precursors as high performance gas sensor. *Cryst.Eng. Comm*. 14, 6654–6658.

[3]. Yang, L., Lin, H. Y., Zhang, Z. S., Cheng, L., Ye, S. Y., and Shao, M. W. (2013). Gas sensing of tellurium-modified silicon nanowires to ammonia and propylamine. *Sens. Actuator*. 177 260–264.

[4]. Guo, J., Zhang, J., Zhu, M., Ju, D., Xu, H, and Cao, B. (2014) High-performance gas sensor based on ZnO nanowires functionalized by Au nanoparticles. *Sens. Actuators B.* 199, 339-345.

[5]. Xua, Q. H., Xua, D. M., Guana, M. Y., Guoa, Y., Qi, Q., and Li, G. D. (2013). ZnO/Al2O3/CeO2 composite with enhanced gas sensing performance. *Sens. Actuators* 177, 1134 -1141.

[6]. Tomer, V. K., and Duhan, S. (2016). Ordered mesoporous Ag-doped TiO2/SnO2 nanocomposite based highly sensitive and selective VOC sensors. *J. Mater. Chem.* 4, 1033–1043.

[7]. Endre, Z. H., Pickering, J. W., Storer, M. K., Hu, W. P., Moorhead, K. T., Allardyce, R., et al. (2011). Breath ammonia and trimethylamine allow real-time monitoring of haemodialysis efficacy. *Physiol. Meas*. 32, 115–130.

[8]. Reyes-Reyes, A., Horsten, R. C., Urbach, H. P., and Bhattacharya, N. (2015). Study of the exhaled acetone in type 1 diabetes using quantum cascade laser spectroscopy. *Anal. Chem.* 87, 507–512.

[9]. Brannelly, N. T., Hamilton-Shield, J. P., and Killard, A. J. (2016). The measurement of ammonia in human breath and its potential in clinical diagnostics. *Crit. Rev. Anal. Chem*. 46, 490–501.

[10]. Philip, J., Punnoose, A., Kim, B. I., Reddy, K. M., Layne, S., Holmes, J. O., et al. (2006). Carrier-controlled ferromagnetism intransparent oxide semiconductors. *Nat. Mater*. 5 298–304.

[11]. Brezesinski, T., Wang, J., Tolbert, S. H., and Dunn, B. (2010). Ordered mesoporous α-MoO_3 with iso-oriented nanocrystalline walls for thin-film pseudocapacitors. *Nat. Mater*. 9, 146–151.

[12]. Greiner, M. T., Chai, L., Helander, M. G., Tang, W. M., and Lu, Z. H. (2013). Metal/Metal-oxide in-terfaces: how metal contacts affect the work function and band structure of MoO3. *Adv. Funct. Mater.* 23, 215–226.

[13]. F. Lai, M. Li, H. Wang, H. Hu, X. Wang, J.G. Hou, Y. Song, Y. Jiang, Thin Solid Films 488, 314 (2005).

[14]. H. Miyake, H. Kozuka, J. Phys. Chem. B 109, 17951 (2005)

[15]. S. Rho, D. Jahng, J.H. Lim, J. Choi, J.H. Chang, S.C. Lee, K.J. Kim, Biosens. Bioelectron. 23, 852 (2008)

[16]. M.T. Tanvir, Y. Aoki, H. Habazaki, Appl. Surf. Sci. 255, 8383 (2009)

[17]. S.M. Mendez, Y. Henriquez, O. Dominguez, L.D. Ornelas, H. Krentzien, J. Mol. Catal. A Chem. 252, 226 (2006)

[18]. A.M. Gaffney, S. Chaturvedi, M.B. Clark Jr., S. Han, D. Le, S.A. Rykov, J.G. Chen, J. Catal. 229, 12 (2005)

[19]. A. Le Viet, M.V. Reddy, R. Jose, B.V.R. Chowdari, S. Ramakrishna, J. Phys. Chem. C 114, 664 (2010)

[20]. A. Le Viet, R. Jose, M.V. Reddy, B.V.R. Chowdari, S. Ramakrishna, J. Phys. Chem. C 114, 21795 (2010)

[21]. Hsin-Yu Lin, Hsien-Chang Yang, Wei-Lin Wang, Synthesis of mesoporous Nb_2O_5 photocatalysts with Pt, Au, Cu and NiO cocatalyst for water splittingCatalysis Today, 2011, 174(1) 106-113.

[22]. Chiu, H. C. &Yeh, C. S. Hydrothermal synthesis of SnO_2 nanoparticles and theirgas-sensing of alcohol. J. Phys. Chem. C 111, 7256–7259 (**2007**).

S.V. Jagtap, et. al. "Ce-doped Nb2O5; Synthesis and Ethanol Sensing Properties." *IOSR Journal of Applied Chemistry (IOSR-JAC)*, 14(9), (2021): pp 16-22.